JOURNAL OF MATERIALS SCIENCE 26 (1991) 5060–5066

Physical properties and microstructure of $YBa_2Cu_3O_{7-y}$ prepared via a simplified nitrate route

Y. FENG, R. E. SMALLMAN, I. P. JONES, F. WELLHOFER
Superconductivity Research Group and School of Metallurgy and Materials, University of Birmingham, P.O. Box 363, Birmingham B15 2TT, UK

A simple nitrate method has been evaluated for producing fine and uniform YBCO powders. A.c. susceptibility measurements have been used to investigate the influence of specific process parameters, i.e. reaction and sintering temperature. The results are correlated with microstructural analyses by SEM and TEM.

1. Introduction

For the preparation of $YBa_2Cu_3O_{7-y}$, several alternatives to the commonly used Y_2O_3–$BaCO_3$–CuO solid state reaction method have been tried, e.g. a sol–gel route [1–3] and a co-precipitation route [4, 5]. The main advantage of these chemical solution techniques is that the final oxide products are finer and more uniformly mixed than those prepared from binary oxides.

The nitrate precursor powders can normally be produced by freeze drying a stoichiometric 123 solution of Y_2O_3, $Ba(NO_3)_2$ and CuO in nitric acid and then precipitating by control of the pH value. The sol–gel method, starting from metal nitrates, involves the use of an organic solvent, ethylene glycol, rather than nitric acid as in the co-precipitation route.

The superconducting properties of the materials processed via these solution routes have proved to be better than those of the material produced via the conventional oxide route [4]. These processes are, however, rather more complicated than the oxide route. Here we have combined the advantages of a solution technique with those of a conventional oxide route by avoiding complexities such as freeze drying or the accurate control of the pH as well as avoiding excessively long milling times and used readily available $BaCO_3$ rather than $Ba(NO_3)_2$. As this route differs significantly from other published nitrate routes, it was necessary to investigate the influence of specific process parameters on the superconducting properties for samples resulting from such a simplified nitrate route.

2. Experimental procedure

Appropriate amounts of Y_2O_3 (99.99% purity), $BaCO_3$ and CuO (both BDH Analar grade) were intimately mixed by hand in suitable proportions to provide the 1–2–3 composition. The 30 g pre-mixed powders were dissolved in 500 ml NHO_3 (69% wt/wt) producing a strong heat reaction. The nitrate solution was boiled and stirred on a hot plate for several hours at roughly 200–250 °C until it became a blue-coloured paste. A small amount of white precipitate remained after the chemical reaction. X-ray diffraction showed that this was undissolved barium nitrate because of its low solubility in acid. The blue paste was then dried overnight at 150 °C and crushed using an agate pestle and mortar. Reaction temperatures of 900, 925, 950 and 975 °C in air were followed by sintering in oxygen at temperatures of 950, 975 and 1000 °C. Reaction times were held at 24 h throughout. All samples were cooled down to room temperature at a rate of 2 °C min^{-1} under flowing oxygen after sintering.

A.c. susceptibility measurements were carried out using a mutual inductance bridge at a measuring field of 5 mOe at a frequency of 1 kHz on samples of dimensions of 6 mm × 2 mm × 2 mm. The powder X-ray diffraction (XRD) data were collected on a Philips diffractometer using CuK_α radiation.

3. Results and discussion

3.1. Influence of reaction temperature

Fig. 1 shows the XRD traces of samples reacted at different temperatures for 24 h and then furnace cooled in air. The sample reacted at 1000 °C shows that a large amount of impurity phases (for example, Y_2BaCuO_5 and $BaCuO_2$) had appeared as indicated by the peaks in the region $2\theta = 27°$–$30°$. Obviously, there is significant decomposition of the sample reacted at 1000 °C ; at the same time some barium-rich liquid phases (most probably $BaCuO_2$) form which appear to degrade significantly the intergranular regions but promote grain growth as evinced by the sample's total melting.

As compared with the 950 °C reacted material, which is essentially single phase, samples reacted at 900, 925 and 975 °C all show some weak peaks of impurity phase in the region $2\theta = 27°$–$30°$. Possibly one reason for these weak peaks is that the reaction temperatures 900 and 925 °C are insufficiently high to

0022–2461/91 $03.00 + .12

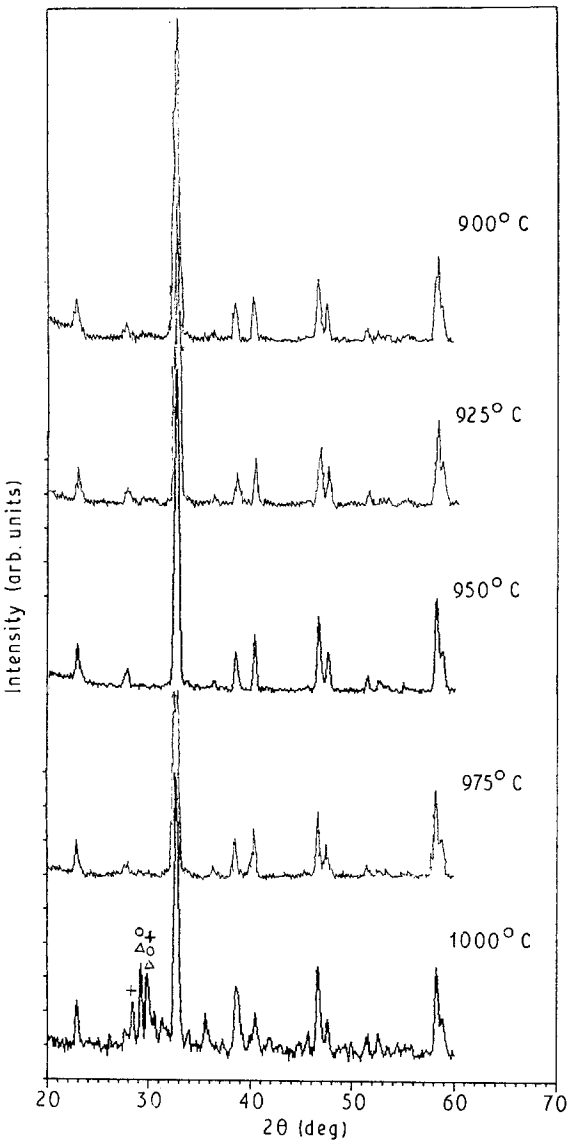

Figure 1 Powder X-ray diffraction traces for the samples reacted at various temperatures for 24 h and then furnace cooled in air. Notice the region $2\theta = 27°–30°$ where peaks from impurity phases are present in the sample reacted at 1000 °C. (○) $BaCuO_2$, (Δ) Y_2BaCuO_y, (+) $BaCuO_3$.

allow the powders to react fully. Another is that the reaction temperature of 975 °C is high enough to cause some decomposition, both processes resulting in impurity phases. Therefore, the best reaction temperature appears to be 950 °C .

The influence of reaction temperature on the particle size of the powders is shown in Fig. 2. As the reaction temperature increases above 900 °C , particles grow with the average particle size increasing from 2–5 μm at 900–925 °C (Fig. 2a, b) to 3–7 μm at 975 °C (Fig. 2d). It is noted that the increase in particle size with increasing reaction temperature is not very significant.

To evaluate the influence of reaction temperature on superconductivity, powders reacted at different temperatures (900, 925, 950 and 975 °C) for 24 h were sintered for 8 h at 950, 975 and 1000 °C, respectively. Fig. 3 shows the effect of the different heat-treatment regimes on the superconducting transitions for these samples. As one would expect, all samples show the onset of superconductivity near 90 K and become bulk-superconductors at some lower temperature. As can be seen from Fig. 3a–c, the details of the diamagnetic transition are strongly dependent on the thermal history of the samples.

In these measurements, the temperature, T^*, at which a sharp rise is observed in the real part of the susceptibility, is interpreted as that for bulk-superconductivity to be established throughout the sample. (At the same temperature a peak is measured in the out-of-phase component of the a.c. susceptibility.) The slowly rising diamagnetic signal measured in the temperature region between T^* and T_c, which is defined as the onset of superconductivity, is believed to be due to the superconducting properties of unconnected or poorly connected grains only. On the basis of such an interpretation, Fig. 3a clearly illustrates that the connectivity in the samples is improved if the reaction temperature is increased from 900 to 950 °C , but that a further increase in temperature at this stage results again in deterioration of the superconducting properties. Fig. 3b and c show a.c. susceptibility data for the material sintered at 975 and 1000 °C . These results always show the sharpest magnetic transition for material initially reacted at 950 °C which suggests that the samples reacted at 950 °C show the best superconducting properties.

The interpretation above of the real susceptibility curves is confirmed by SEM observation as shown in Figs 4 and 5. After 8 h sintering at 950 °C (Fig. 4) the samples reacted at 900 and 925 °C show an undefined morphology consisting of poorly connected small grains (2–5 μm) because the reaction temperature is insufficiently high. In contrast, the sample reacted at 950 °C exhibits larger, more defined grains between which a better connection is formed. The sample reacted at 975 °C has larger grains with better contacts than those of the samples reacted at 900 and 925 °C, but is still poorer than the sample which was reacted at 950 °C.

3.2. Influence of sintering temperature

The influence of sintering temperature on samples previously reacted at different temperatures can be seen from Fig. 6. Fig. 6b–d show that sintering at higher temperature results in a shorter tail and a sharper transition in the real part of the susceptibility curve. Sintering at 1000 °C appears to give the best magnetic property. This is probably because sintering at higher temperatures promotes grain growth and improves the contact between grains as evinced by the scanning electron micrographs (Fig. 5) which show a denser material consisting of larger grains with better contacts in the intergranular regions as compared with those in Fig. 4.

However, it is reported that sintering at higher temperature (1000 °C) yields the barium-rich liquid phase which degrades intergranular regions [6]. By using X-ray diffraction analysis, the impurity phase levels in each sample sintered at 1000 °C have been determined (Fig. 7). Compared with the X-ray traces shown in Fig. 1, no impurity peaks have been found in the sample reacted at 950 °C even after sintering at

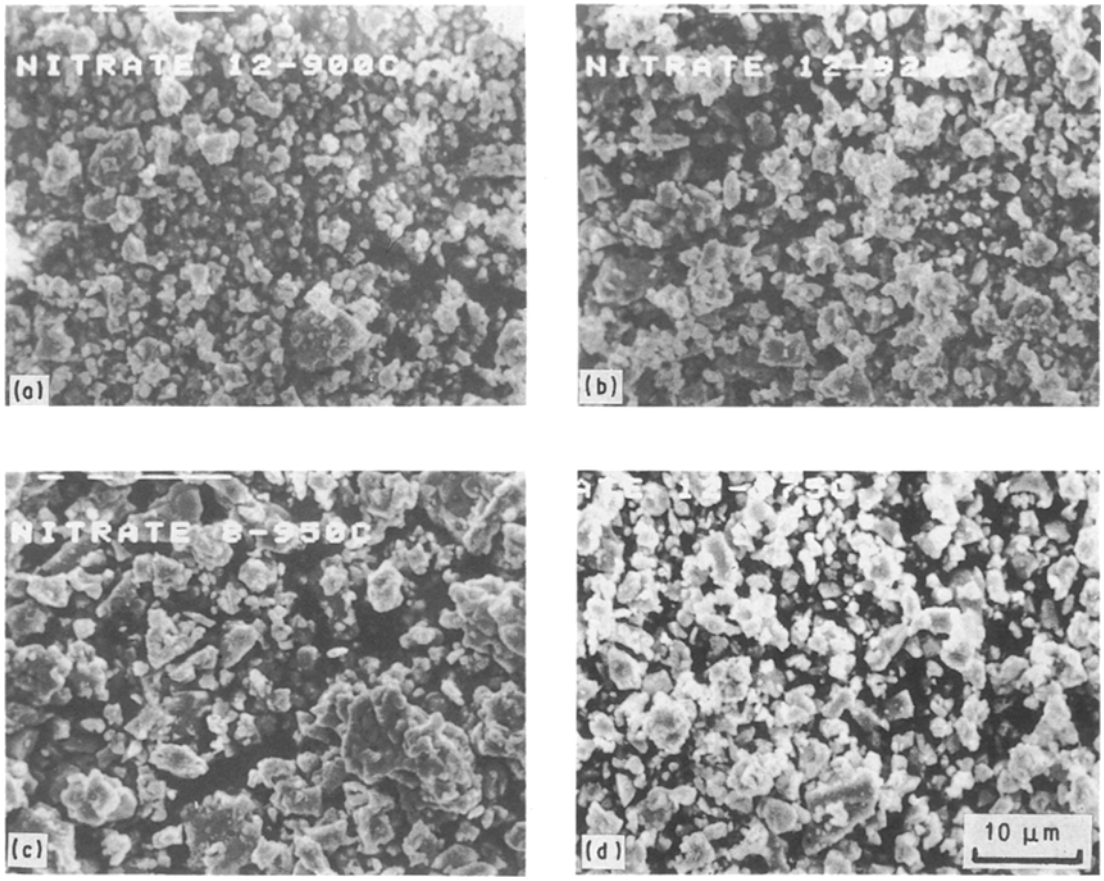

Figure 2 Scanning electron micrograph showing the particle size of the powders reacted at different temperatures (for 24 h); (a) 900 °C, (b) 925 °C, (c) 950 °C and (d) 975 °C.

1000 °C for 8 h (Fig. 7c). This is in contradiction to the results of the samples prepared via the oxide route which normally show significant grain growth and a considerable amount of barium-rich impurity phase after sintering at 1000 °C [6]. In the sample reacted at 975 °C, some weak peaks from impurity phases occurred after sintering at 1000 °C (Fig. 7d).

It is interesting to note (Fig. 6a) that two clear plateaux in the real part of the susceptibilty were found in the sample which was reacted at 900 °C and sintered at 1000 °C for 8 h. This may indicate that two superconducting phases have occurred in this sample as suggested by multiple loss-peaks in the imaginary part of the susceptibility (Fig. 8). It would be interesting to know whether the 60 K phase is oxygen-deficient 123 or an impurity phase.

X-ray diffraction revealed that a large amount of impurity phases, mainly $BaCuO_2$ and Y_2BaCuO_5,

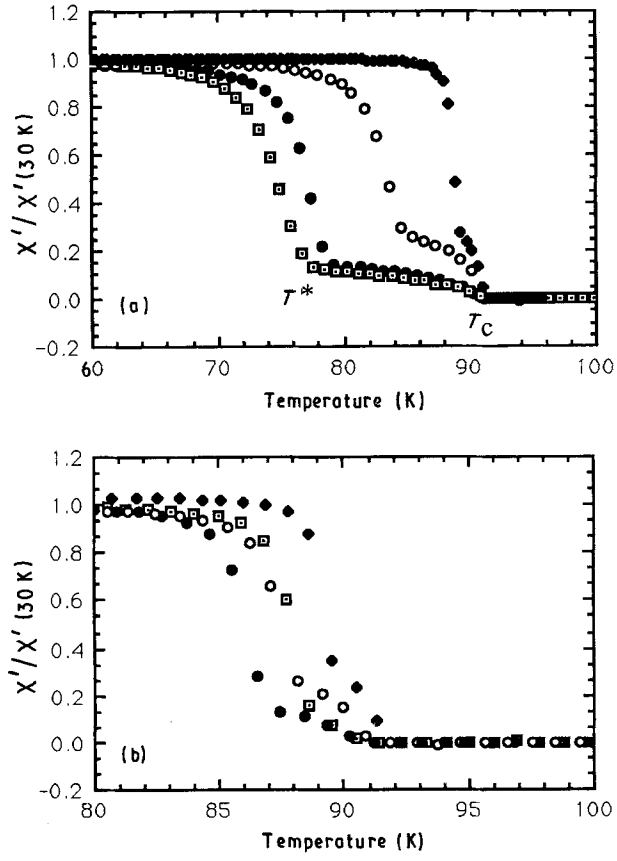

Figure 3 Susceptibilities plotted against temperature, showing the influence of reaction temperature (⊡, 900; ●, 925; ◆, 950; ○ 975 °C; for 24 h). All samples sintered for 8 h after reaction at (a) 950 °C, (b) 975 °C and (c) 1000 °C.

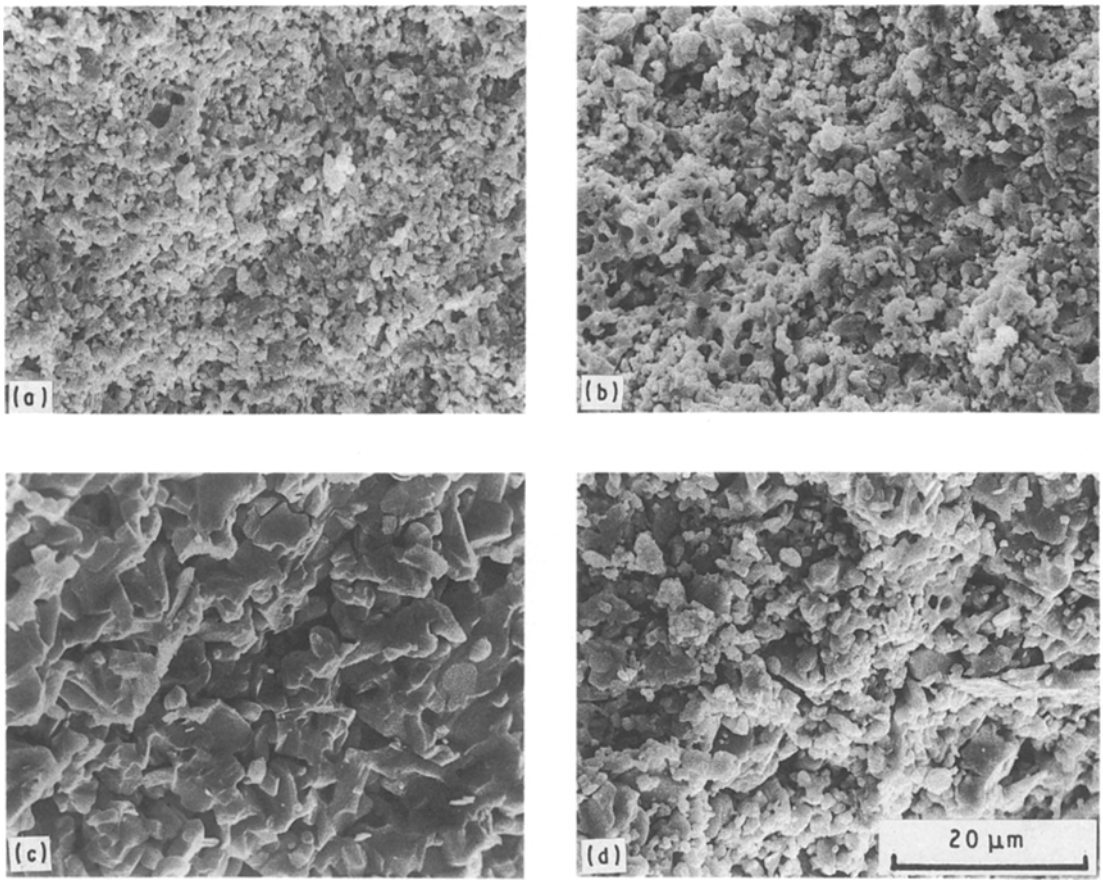

Figure 4 Scanning electron micrographs of the samples reacted at different temperatures showing different grain morphologies. (All samples sintered at 950 °C/8 h after reaction.) (a) 900 °C, (b) 925 °C; (c) 950 °C and (d) 975 °C.

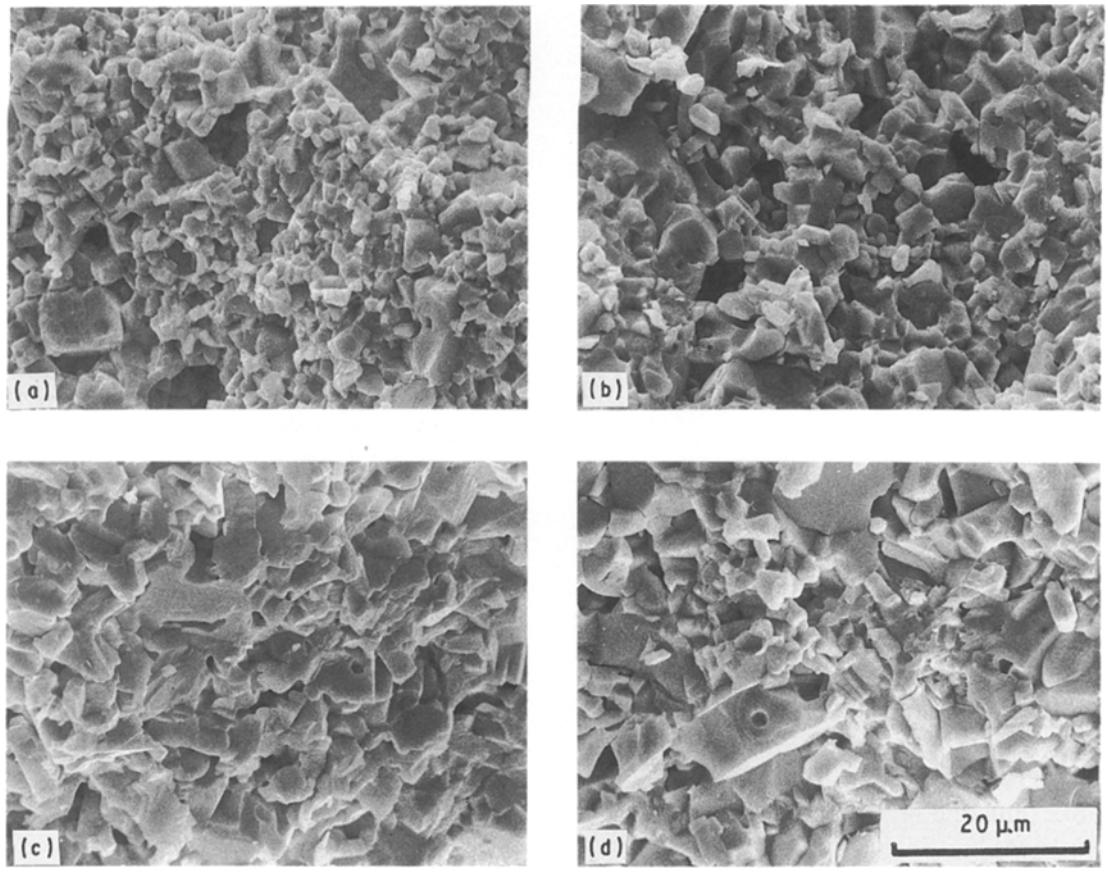

Figure 5 Scanning electron micrographs of the samples reacted at different temperatures showing different grain morphologies. (All samples sintered at 1000 °C/8 h after reaction.) (a) 900 °C, (b) 925 °C; (c) 950 °C and (d) 975 °C.

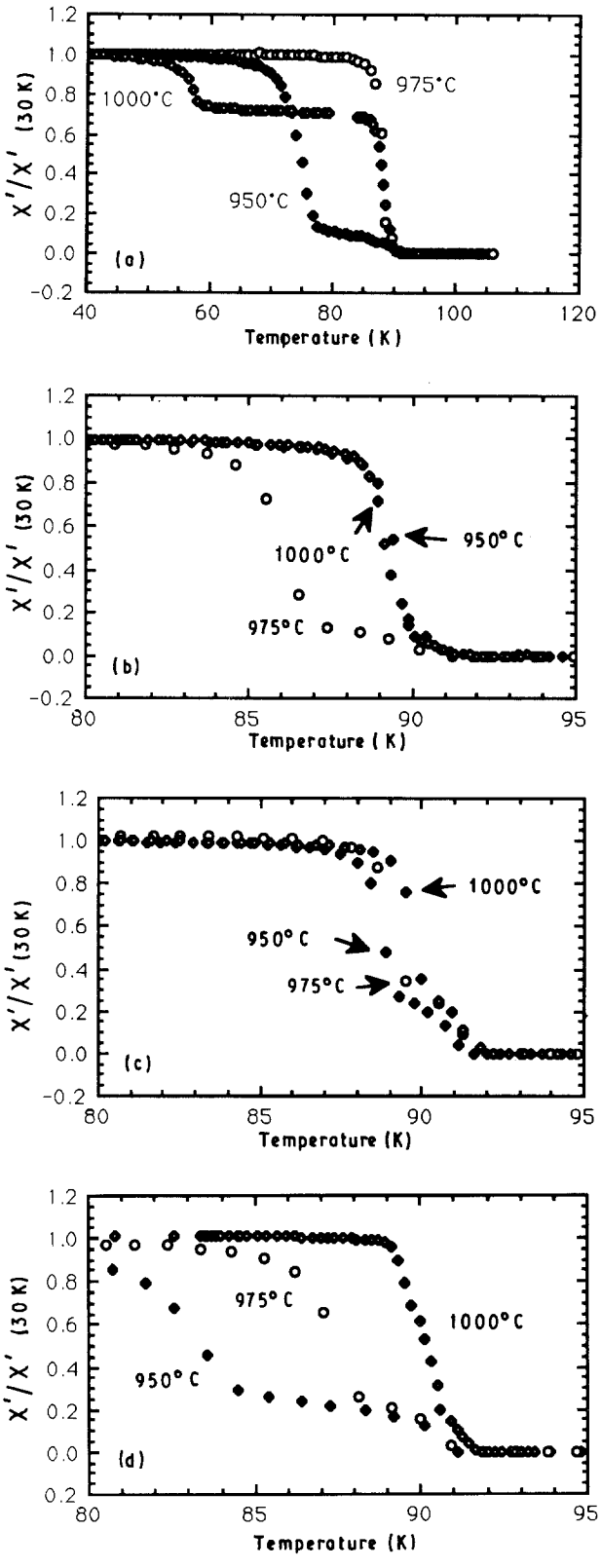

Figure 6 Susceptibilities showing the influence of sinter and reaction temperatures. Sintering was at 950, 975 and 1000 °C for 8 h. Samples were reacted preliminarily for 24 h at (a) 900 °C, (b) 925 °C, (c) 950 °C and (d) 1000 °C.

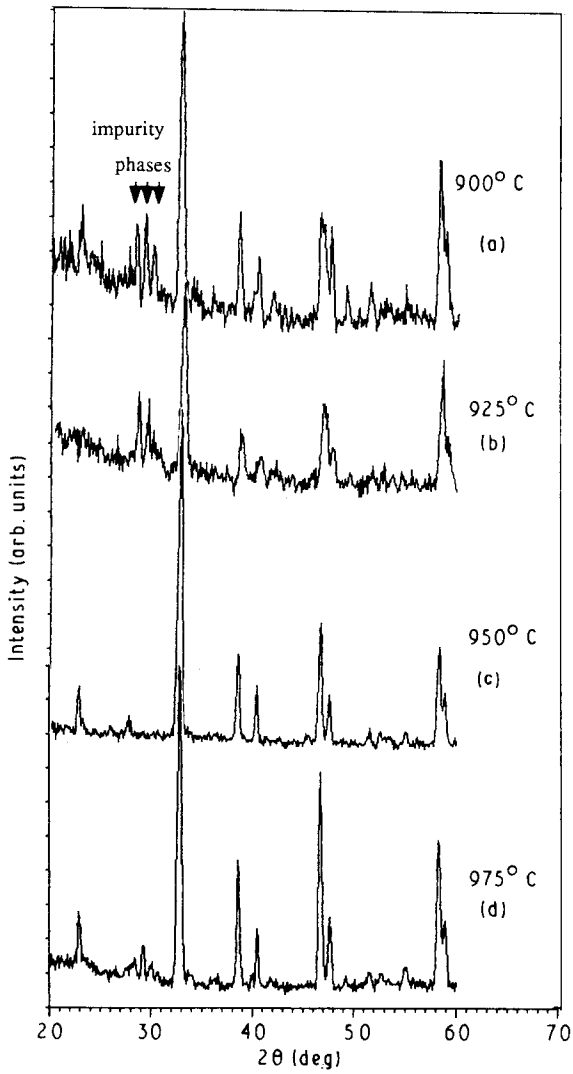

Figure 7 X-ray diffractometer traces for the samples sintered at 1000 °C for 8 h. Notice the impurity phase level in the region $2\theta = 27°–30°$.

exists in the sample which was reacted at 900 °C and sintered at 1000 °C for 8 h (Fig. 7a), probably due to incomplete reaction at 900 °C and a higher subsequent temperature sintering at 1000 °C. The crystal lattice parameters for the 123 phase have been measured using X-ray diffraction as shown in Table I. It is clear from these results that the lattice parameters of Sample b have changed significantly after further sintering at 1000 °C for 8 h as compared with the results of Sample a, which was only reacted at 900 °C for 24 h. The changes in the lattice parameters as a consequence of sintering at 1000 °C lead to a reduction of the orthorhombic ratio (b/a) from 1.017 to 1.014, indicating that Sample b is oxygen deficient. Therefore, some oxygen-deficient orthorhombic II phase ($T_c = 60$ K) should have been produced, as suggested by the susceptibility measurement which shows two transitions at 91 and 60 K, respectively. Possibly, the abundant occurrence of impurity phases in this sample may be responsible for its oxygen deficiency because oxygen is needed for the formation of these impurity oxide phases. Although Sample c has also been sintered at 1000 °C for 8 h, it still shows a large orthorhombic ratio ($b/a = 1.020$), only a small amount of impurity phase and a single transition in its susceptibility measurement at 91 K.

Many spherical pores have been found in Sample b both by SEM (Fig. 5a) and optical examination (Fig. 9). Two possible reasons for these spherical pores may be (1) sintering contraction or (2) formation of gases. Because of these small grains' size after reaction at 900 °C, a strong shrinkage occurs when these small

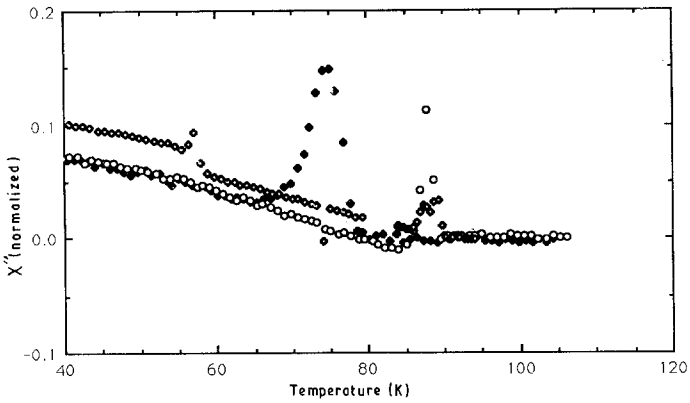

Figure 8 The imaginary part of the susceptibility for the sample reacted at 900 °C and sintered at 1000 °C showing two loss peaks which implies that two superconducting phases (T_c = 90 and ~60 K) occur in this sample. Sintering temperature: (◆) 950 °C, (○) 975 °C, (◇) 1000 °C.

TABLE I The lattice parameters for the 123 phase with varying treatment conditions measured using X-ray diffraction

Sample	Treatment conditions	Crystal parameters (nm)		
		a	*b*	*c*
a	reaction: 900 °C/24 h	0.381 34	0.387 74	1.164 00
b	reaction: 900 °C/24 h, sinter: 1000 °C/8 h	0.382 79	0.387 97	1.171 50
c	reaction: 975 °C/24 h, sinter: 1000 °C/8 h	0.381 67	0.389 20	1.168 30

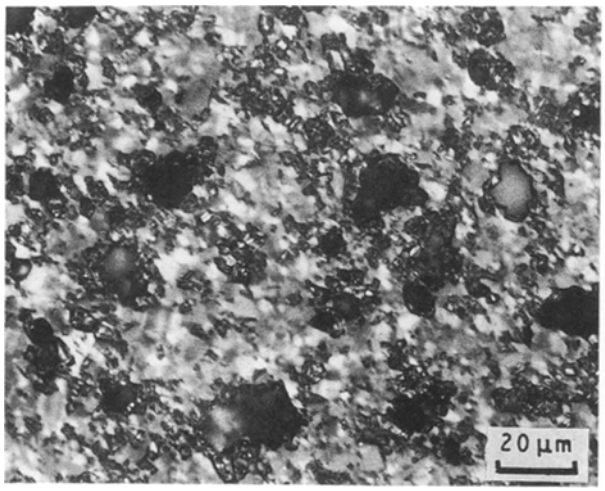

Figure 9 Optical micrograph of Sample b (reacted at 900 °C/24 h and sintered at 1000 °C/8 h) showing the appearance of abundant spherical pores, possibly due to gas formation because of incomplete reaction at 900 °C.

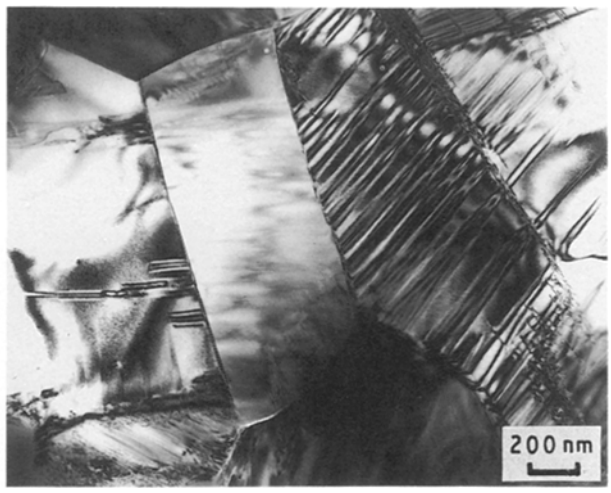

Figure 10 Typical transmission electron micrograph of Sample b (reacted at 900 °C/24 h and sintered at 1000 °C/8 h) showing some twinned and untwinned grains. The untwinned grains may be oxygen deficient.

grains are suddenly sintered at a much higher temperature (1000 °C). It seems that the second reason is more likely. Some of the $Ba(NO_3)_2$ and perhaps some unreacted $BaCO_3$ may not be fully dissolved during the chemical reaction as evinced by the white precipitates. After reaction at 900 °C, some nitrates may not be fully decomposed and still remain in the material because the temperature is insufficiently high. During sintering at 1000 °C, these incompletely reacted nitrate precipitates (after being pressed to discs) decomposed with the formation of CO_2 or N_2.

Because Sample b (900 °C reaction and 1000 °C sintering) behaves in a different way from the others, it was also examined using TEM. The overall microstructure seems similar to the common run of 123 materials, but with more frequent appearance of untwinned areas which are possibly the oxygen-deficient orthorhombic II phase (Fig. 10). However, several untwinned grains have been examined at the [0 0 1] beam diffraction and no 1/2, 0, 0 superlattice spots have been found. Some spherical yttrium-rich second phase (Y_2BaCuO_{5-y} as revealed by EDX) have been found clustered in some regions which implies that this sample has more impurity phase than the others (Fig. 11). This is consistent with the results of the XRD which show a large amount of impurity phase.

Holes have been found inside grains in some regions; this has never been seen before in any of the samples made via the oxide route and the nitrate route (Fig. 12). A possible reason for these holes is that some precipitates drop out of the matrix during TEM specimen preparation. These precipitates, again, could result from incomplete reaction at the lower temperature (900 °C).

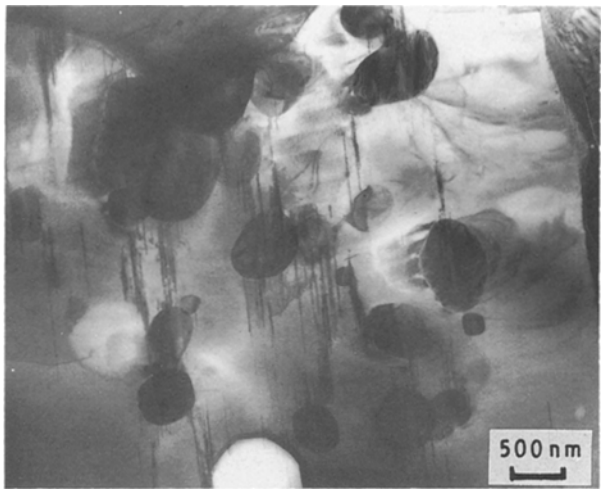

Figure 11 Transmission electron micrograph of Sample b (reacted at 900 °C/24 h and sintered at 1000 °C/8 h) showing the occurrence of a large amount of second phase (Y_2BaCuO_{5-y} as shown by EDX).

Figure 12 TEM microstructure of Sample b (reacted at 900 °C/24 h and sintered at 1000 °C/8 h) showing some holes inside grains (as indicated by arrows) possibly due to some precipitates dropping out of the matrix during TEM specimen preparation.

The density data from samples with varying reacting and sintering temperatures are shown in Table II. Clearly, the densities of all samples reacted at various temperatures increase with sintering temperature (1000 °C). These denser microstructures show sharp diamagnetic transitions as has been shown in Fig. 6. TEM investigation revealed that most grain boundaries of the materials made via the nitrate route are clean. Overall, these results suggest that the nitrate route can produce easily a denser material with finer grain size and good grain contacts under proper processing conditions and these may lead to a higher critical current density capacity than is possible with the more usual oxide precursors.

TABLE II The density data from samples with varying reacting and sintering temperatures (% theoretical values)

Sintering temperature (°C)	Reacting temperature (°C)			
	900	925	950	975
950	68.6	67.6	80.0	72.7
975	81.6	77.9	81.5	75.5
1000	85.7	83.6	86.0	92.7

4. Conclusions

1. Reaction of the nitrate precursors at 900–925 °C is incomplete and some nitrate precipitates and impurity phases remain. At 1000 °C, a significant decomposition occurs resulting in a large amount of impurity phase. Reaction at 950 °C produces a single 123 phase.

2. Sintering at higher temperature (975–1000 °C) promotes grain growth and improves the contacts between grains. If the sample is preliminarily reacted at 950 °C, a 123 single phase can still be obtained by 1000 °C sintering. Incomplete reaction at 900–925 °C and subsequent high-temperature sintering (1000 °C) results in an abundant occurrence of impurity phases leading to a strong volume shrinkage and oxygen deficiency in the bulk material.

3. The use of the simplified nitrate route can yield fine and uniform powders and thus a denser material consisting of smaller grains and better intergranular contacts can be obtained. It is expected that a higher critical current, J_c, can be more easily obtained using this route than by the more usual oxide precursor materials.

References

1. G. ARCANGELI, R. VATTERONI and R. FAVA, presented at "First European Workshop on High T_c Superconductors and Potential Applications", Genova, Italy (1987).
2. M. NAGANO and M. GREENBLATT, *Solid State Commun.* **27** (1988) 595.
3. E. A. HAYRI, M. GREENBLATT, K. V. RAMANUJACHARY and M. NAGANO, *J. Mater. Res.* **4** (1989) 1099.
4. P. BARBOUX, J. M. TARASCON, L. H. GREENE, G. W. HULL and B. G. BAGLEY, *J. Appl. Phys.* **63** (1988) 2725.
5. A. BRIGGS, I. E. DENTON, R. C. PILLAR, T. E. WOOD and G. FERGUSON, *Br. Ceram. Proc.* **40**(3) (1988) 37.
6. D. S. GINLEY, E. L. VENTURINI, J. F. KWAK, R. J. BAUGHMAN and B. MOROSIN, *J. Mater. Res.* **4** (1989) 496.

Received 2 August
and accepted 20 December 1990